RESEARCH ARTICLE | APRIL 26 2023

Active steering of omni-droplets on slippery cross-scale arrays by bi-directional vibration

Sizhu Wu ; Le Xiang ; Zhang Yiyuan (张亦元) ; Shaojun Jiang ; Chuanzong Li; Zhipeng Zhao; Zhang Yiyuan (张艺媛); Qiyu Deng ; Shuting Xie; Yunlong Jiao ; Chao Chen; Zhaoxin Lao ; Liqiu Wang

Appl. Phys. Lett. 122, 174101 (2023)
https://doi.org/10.1063/5.0146217

Applied Physics Letters ARTICLE scitation.org/journal/apl

Active steering of omni-droplets on slippery cross-scale arrays by bi-directional vibration

Cite as: Appl. Phys. Lett. **122**, 174101 (2023); doi: 10.1063/5.0146217
Submitted: 11 February 2023 · Accepted: 9 April 2023 ·
Published Online: 26 April 2023

View Online Export Citation CrossMark

Sizhu Wu,[1,2] Le Xiang,[1] Yiyuan Zhang (张亦元),[3,a)] Shaojun Jiang,[3] Chuanzong Li,[4] Zhipeng Zhao,[3] Yiyuan Zhang (张艺媛),[3] Qiyu Deng,[3] Shuting Xie,[3] Yunlong Jiao,[5] Chao Chen,[6] Zhaoxin Lao,[1,2] and Liqiu Wang[7,a)]

AFFILIATIONS

[1]School of Instrument Science and Opto-Electronics Engineering, Hefei University of Technology, Hefei 230009, China
[2]Anhui Province Key Laboratory of Measuring Theory and Precision Instrument, Hefei University of Technology, Hefei 230009, China
[3]Department of Mechanical Engineering, University of Hong Kong, Hong Kong, China
[4]School of Computer and Information Engineering, Fuyang Normal University, Fuyang 236037, China
[5]Institute of Tribology, Hefei University of Technology, Hefei 230009, People's Republic of China
[6]College of Materials Science and Engineering, Hefei University of Technology, Hefei 230009, China
[7]Department of Mechanical Engineering, Hong Kong Polytechnic University, Hong Kong, China

[a)]**Authors to whom correspondence should be addressed:** yyz2017@hku.hk and liqiu.wang@polyu.edu.hk

ABSTRACT

Directed droplet manipulation is paramount in various applications, including chemical micro-reaction and biomedical analysis. The existing strategies include some kinds of gradients (structure, inherent wettability, and charge density), whereas they suffer from several limitations, such as low velocity, limited volume range, poor durability, and inefficient environmental suitability. Moreover, active bi-directional reversal of omni-droplets remains challenging because one kind of microstructure at a single scale cannot acquire two kinds of net results of mechanical interaction. Herein, we report an active and directional steering of omni-droplets utilizing bi-directional (vertical and horizontal) vibration on slippery cross-scale structures consisting of macro millimeter-scale circular arc arrays and micro/nanometer-scale slant ratchet arrays, which are fabricated by femtosecond laser patterned oblique etching and lubricant infusion. The physical mechanism of active droplet steering lies in the relative competition between the forces under vertical and horizontal vibration, which mainly arise from the circular arc arrays and slant ratchet arrays, respectively. Various steering modes, including climbing and programmable manipulation, can be realized. Our work is applicable to a wide range of potential applications, including circuit on/off and droplet-based chemical micro-reaction, particularly in the field of high-throughput omni-droplets operation.

Rectified transport of omni-droplets plays a critical role in applications, such as digital microfluidics,[1] water harvesting,[2,3] chemical reaction,[4,5] and biomedical analysis.[6–8] Typical transport strategies include those that utilize gradients on the substrate including structure,[9–14] inherent wettability,[15,16] and charge density.[17,18] These strategies have some advantages like long transport distance, moderate velocity, and good durability. However, the direction of droplet motion could not be switched flexibly and reversibly to acquire a steering transport along opposite directions.

Recently, a kind of Araucaria leaf has been found to transport liquids with varying surface tension in a steering way featured with the spreading of low-surface-tension liquids along the tilting direction of ratchets while high-surface-tension liquid is moving along the opposite direction.[9] This phenomenon counts on the inherent properties of liquids. However, the objects to be controlled can only be continuous liquids, and the active controllability is not good enough to acquire versatile and programmable manipulation of droplets. Additionally, a steerable transport of droplet impinging on heated concentric microgroove arrays is reported, where the substrate temperature determines the direction of droplet bouncing.[19] Nevertheless, the high temperature is not applicable to some applications that cannot hold several hundred temperatures. First proposed by Chaudhury *et al.*,[20–22] mechanical vibration could serve as a stimulating strategy for droplet transport and have a wide range of advantages, including no-contamination, facileness, as well as robustness and durability. Zhang *et al.*[6] demonstrated a vibration-actuated platform to achieve the rectified motion of droplets

resulting from the relative competition between the asymmetric adhesive resistance and the inertial driving force. However, it is still challenging to realize the high-performance active steering of omni-droplets because the widely used surface/interface structures are solely at a single scale, which makes it hard to achieve two sorts of net mechanical interaction along the opposite directions.

Here, we show an unexpected active directional steering of omni-droplets by bi-directional mechanical vibration on the slippery cross-scale arrays (SCSAs), which consist of millimeter-scale circular arc arrays and micro/nanometer-scale slant ratchet arrays. Droplet motion on the SCSA exhibits a forward direction under vertical vibration and a backward direction under horizontal vibration. The transport capacity, including volume range and velocity, could be tailored flexibly across a wide range by regulating the vibration parameters, such as frequency and amplitude. Moreover, the real-time and programmable steering of multi-droplets could be achieved by dynamically manipulating vibration frequency. The physical mechanism responsible for steering transport lies in the relative competition between two effects arising from the circular arc arrays and slant ratchet arrays. Finally, to demonstrate the potential application of omni-droplets steering, we design and fabricate a circuit that can be switched on/off reversibly and programmatically by utilizing the directional steering motion of conductive droplets.

In Fig. 1(a), the SCSA manifests a capacity of active droplet steering. Under vertical vibration, the droplet is propelled along the forward direction, while the droplet is actuated along the backward direction under horizontal vibration. We define the curvature direction of the arcs from the center to the outer as the forward direction and the tilting direction of the ratchets as the backward direction. This kind of slippery cross-scale arrays is designed and prepared by patterned scanning of femtosecond laser oblique focusing.[23–26] Afterward, the slippery lubricant (e.g., silicone oil) is infused into the arcs microgrooves to achieve the effect of slippery liquid-infused porous surfaces (SLIPS).[27] In the top view, the circular arcs are characterized by the curvature radius (R) of ~6 mm [Fig. 1(b)]. The apparent optical change could be observed in the top view due to the infused lubricant. In the side view, the micro-ratchet arrays are featured with the groove depth (D) of ~72 μm, tip-to-tip pitch (P) of ~118 μm, and tilting angles of the front (α_1) and rear (α_2) plane of a single ratchet of ~65° and ~33°, respectively [Fig. 1(c)]. After infusing the silicone oil, a thin oil film could be observed from the side view [Fig. 1(c)].

In Fig. 1(d) and Movies S1 and S2 (supplementary material), under vertical vibration, the droplet is propelled in the forward direction, whereas the droplet moves along the backward direction under horizontal vibration. We also investigate the droplet steering on the SCSA by utilizing diverse liquids [Fig. 1(e)]. All these liquid droplets manifest an apparent active steering behavior, which shows that the SCSA works for omni-droplets, arising from the omniphobicity of the SLIPS effect.

The steering capacity of droplets on the SCSA, such as volume range and transport velocity, could be regulated precisely by finely

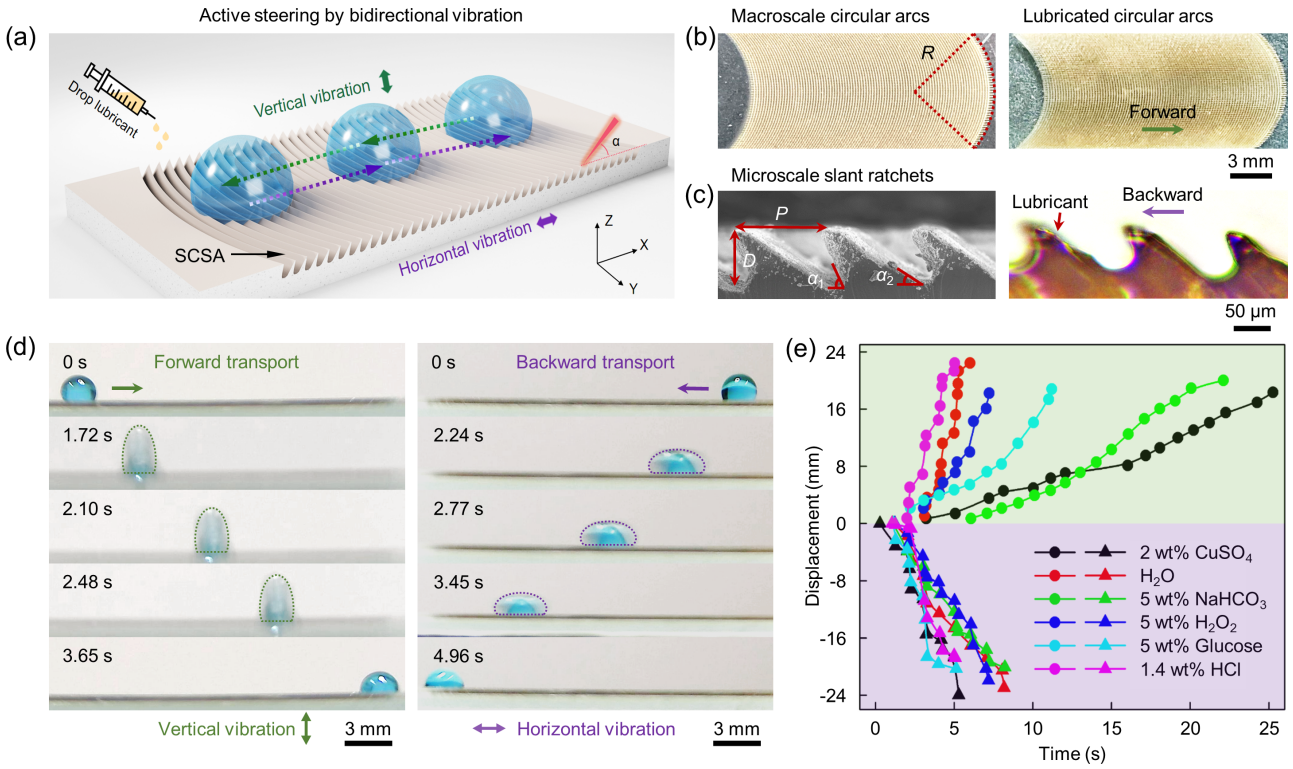

FIG. 1. (a) Schematic illustration of the directional droplet steering driven by mechanical vibration on the SCSA. (b) Optical images of circular arc arrays before and after infusing the lubricant at a macro scale. (c) The scanning electron microscopy (SEM) image of slant ratchet arrays. The side optical view indicates a thin film of the infused lubricant. (d) Steering transport of water droplets on the SCSA. (e) Transport displacement of various droplets vs time.

tuning vibration parameters. Multiple droplets with different volumes (10–60 μL) are deposited on the SCSA utilizing vibration with various frequencies (20–70 Hz) under vertical vibration [Fig. 2(a)]. With the increase in the droplet volume, the range of vibration frequency to enable the droplets transport decreases from ~37 to ~13 Hz, which might be caused by the increased resistance force from the increased gravity of droplets. In contrast, there exist two regimes for efficient droplet transport under horizontal vibration [Fig. 2(b)]. To further investigate the effect of vibration frequency on droplet transport, we measure the average velocity of droplets under different frequencies [Figs. 2(c) and 2(d)]. Under vertical vibration, there are multiple peak frequencies for the local maximum transport velocity of droplets with different volumes (10, 20, and 60 μL). The appearance of multiple peak frequencies may come from the change in the length of the contact line as the droplet is compressed and released during vertical vibration [Fig. 2(c)]. In contrast, the horizontal vibration results in two peak frequencies for the local maximum transport velocity of droplets with different volumes (10, 20, and 60 μL). There are only two peak frequencies that are relevant to the system resonance resulting from the approximate frequency-doubled relationship [Fig. 2(d)].

Under vertical vibration, there is an optimum vibration amplitude for a fixed vibration frequency corresponding to the highest transport speed. For example, the speed reaches ~11, ~15, and ~16 mm/s with droplet volumes of ~60, ~20, and ~10 μL at the amplitudes of ~13 Vpp (Voltage peak-peak), ~14 Vpp, and ~19 Vpp, respectively [Fig. 2(e)]. However, under horizontal vibration, the

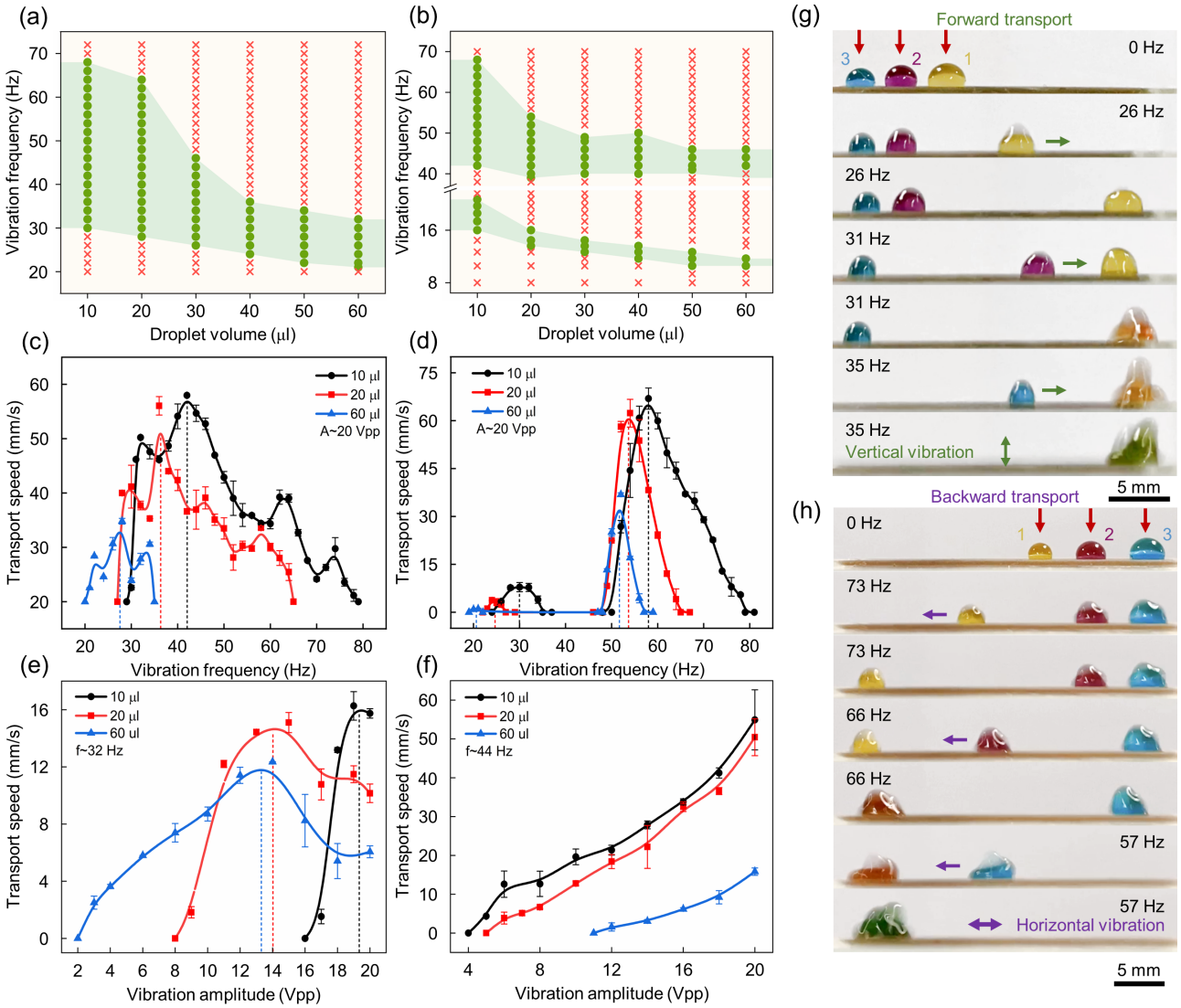

FIG. 2. (a) and (b) The vibration frequency for droplets with different volumes. (c) and (d) Controllable manipulation of droplets transport velocity with different volumes by modulating the vibration frequency. (e) and (f) The transport velocity of droplets with different volumes under bi-directional vibration as a function of the amplitude. (g) and (h) Programmable and sequential steering manipulation of multiple droplets with different volumes.

transport speed of droplets with different volumes (10, 20, and 60 μL) increases monotonically from 0 to ~55, ~50, and ~14 mm/s with the increase in vibration amplitudes (4–20 Vpp) [Fig. 2(f)].

We design and conduct a programmable, real-time, and sequential transport of multi-droplets with different volumes. Under vertical vibration, droplets named "1," "2," and "3" with a volume of ~14, ~8, and ~6 μL, respectively, deposited on the SCSA are transported sequentially to achieve a programmed liquid mixing. At the frequency of ~26 Hz, droplet 1 is transported in a forward direction while droplets 2 and 3 are pinned. Afterward, the frequency is tuned to ~31 and ~35 Hz to drive droplets 2 and 3 to reach the destination in sequence to form a large droplet [Fig. 2(g) and Movie S3 (supplementary material)]. Similarly, under horizontal vibration, three droplets are transported sequentially in the backward direction under the ladder-changing frequency to achieve a programmable and sequential transport [Fig. 2(h) and Movie S4 (supplementary material)].

The wide range of liquid types arises from the infused lubricant, which forms a molecule-level smooth and chemically inert oil film. As the thickness of the infused lubricant is thin, the SLIPS effect is weak and the resistance force is too large to acquire an efficient motion. When the thickness of the lubricant is thick, the underlying substrate characterized by the cross-scale macro-/microstructures is covered by the infused lubricant so that efficient directional droplet transport is abandoned. To prove this, we utilize the SCSA with different lubricant thicknesses by controlling the spinning time of the infused oil to measure the transport velocity of a droplet at the constant vibration condition (f ~60 Hz and A ~20 Vpp). The maximum transport velocity is ~13 and ~16 mm/s, respectively, under vertical and horizontal vibration [Figs. 3(a) and 3(b)].

We also design and conduct a series of experiments to study the grade-ability of droplets on the SCSA. The transport speed of droplets on the SCSA under vertical and horizontal vibration both decreases with the increase in climbing angle as a result of the increased gravity component serving as an extra resistance force [Figs. 3(c) and 3(d)].

To demonstrate the steering capacity of omni-droplets on the SCSA, we utilize a series of liquids with varying viscosity and surface tension by mixing water with glycerin or ethanol. The transport speed of droplets with different volumes (10 and 20 μL) decreases with the increase in glycerin concentration from 0 to ~60% under both vertical and horizontal vibrations [Figs. 3(e) and 3(f)]. Similarly, the transport speed of droplets with different volumes decreases with the increase in the ethanol concentration, namely, the surface tension [Figs. 3(g) and 3(h)]. It turns out that the SCSA is applicable to a wide range of droplets with high-viscosity and low-surface-tension values.

To elucidate the underlying mechanism of droplet steering on the SCSA actuated by bi-directional vibration, we first examined the dynamic changes in droplet shape under vertical and horizontal vibrations, respectively. Under vertical vibration, an inertial force arising from the relative motion between the droplet and the substrate compresses and stretches the droplet periodically, which forces the droplet into a spreading and recoiling state [top two schematic panels and insets in Fig. 4(a) and Movie S5 (supplementary material)]. In contrast to vertical vibration, the inertial forces arising from horizontal vibration are parallel to the direction of droplet transport leading to a similar state that the droplet seems to be pulled to the left and to the right.[6] From the macro side views, there are no obvious differences in the dynamic shape of droplets [top two schematic panels and insets in Fig. 4(d) and Movie S6 (supplementary material)].

We then resorted to a mechanical analysis to probe how the dynamic changes in the droplet shape affect the pinning and releasing of liquid corners for directional steering. Capillary forces of liquid

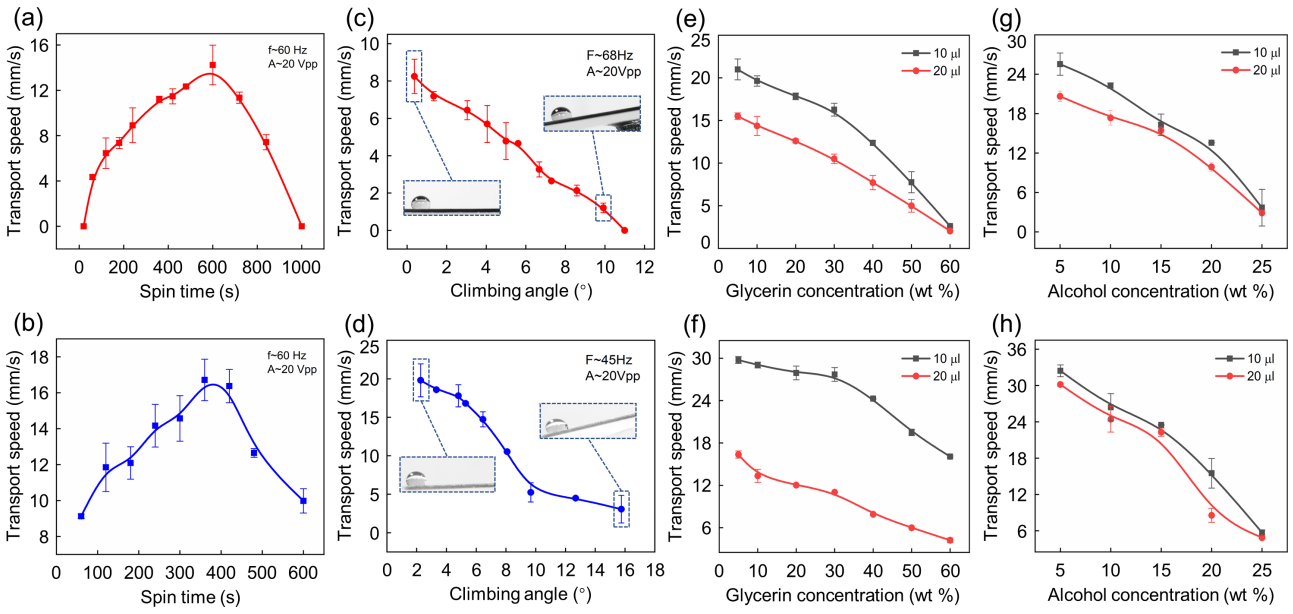

FIG. 3. (a) and (b) The transport speed of droplets is a function of the spin time of the infused lubricant, which results in different lubricant thicknesses. (c) and (d) With the increase in tilting angle of the SCSA, the transport speed of droplets on the horizontally- and vertically vibrated SCSA both decreases. (e) and (f) The transport velocity of droplets with different volumes under bi-directional vibration as a function of the viscosity. (g) and (h) The transport speed of droplets with different volumes under bi-directional vibration is a function of surface tension.

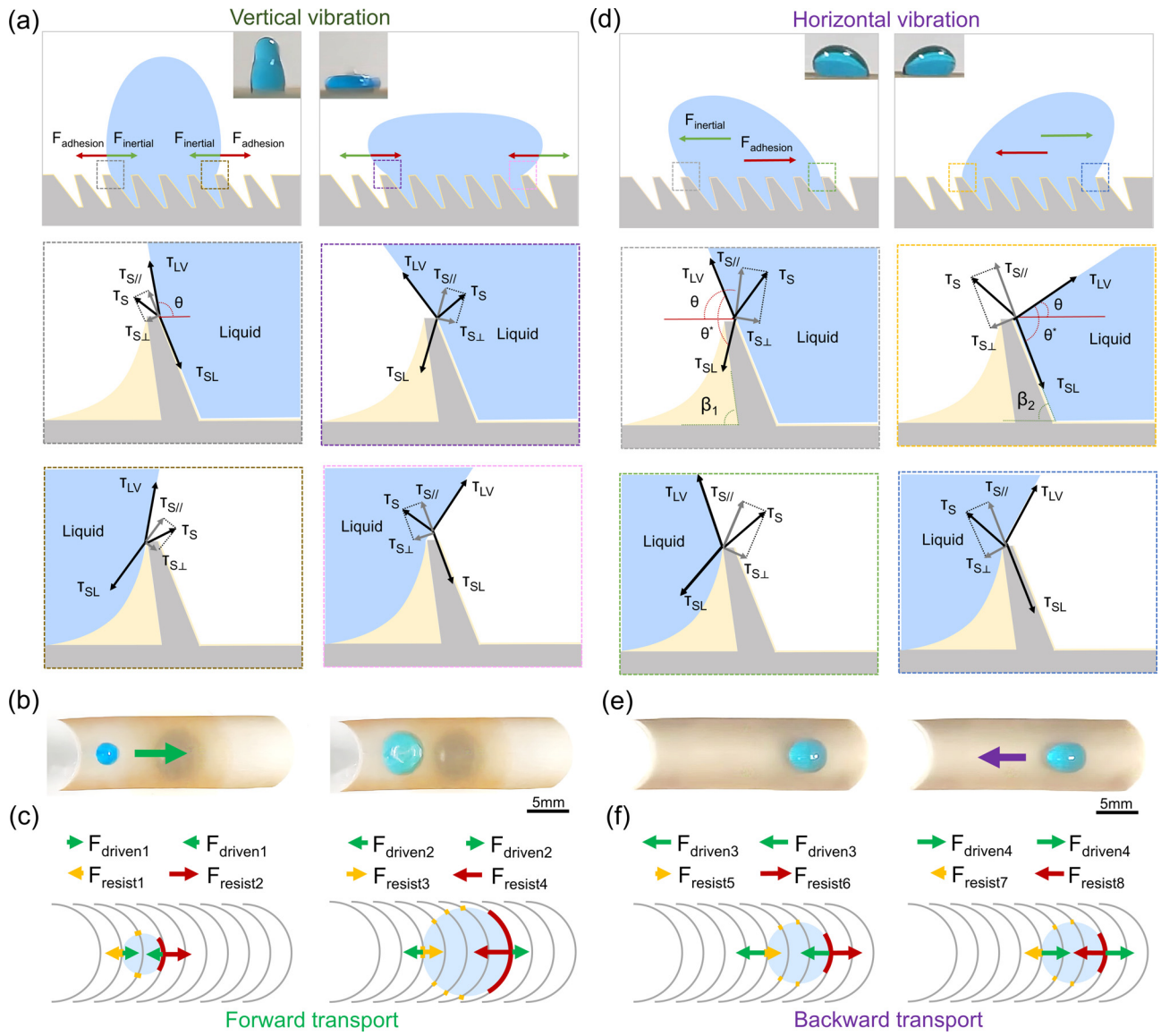

FIG. 4. (a) Mechanical models of dynamic contact angles near the three-phase contact lines. (b) and (c) In the top view, an apparent difference in contact lines could be observed due to the circular arc arrays. (d)–(f) While under horizontal vibration, the droplet motion is determined mainly by the slant ratchet arrays.

corners are analyzed instead of utilizing surface tensions on contact lines due to physical reasons.[28–30] In the stretching state of the droplet actuated by vertical vibration, capillary forces include τ_{SL} and τ_{LV} based on the cohesion of liquid droplets, and τ_S based on the adhesion between the SCSA substrate and the liquid droplet. It should be obviously noted that the liquid corner of the droplet always moves along the direction parallel to the substrate interface so that capillary force τ_S is prioritized to be broken into normal and tangential components $\tau_\perp$ and $\tau_{S//}$, which is perpendicular and parallel to the substrate. In the normal direction, there exists a force balance: $\tau_{S\perp} = \tau_{LV}\cos(\theta^*_+ - \pi/2)$, where θ^*_+ represents the dynamic contact angle during the recoiling process of the droplet. Obviously, the force balance in the parallel direction determines the droplet motion: $\tau_{S//} = \tau_{SL} + \tau_{LV}\cos\theta^*_+$. As the droplet is actuated by vertical vibration and experiences the shape change due to the vertical inertial force, there exists a relatively modest change in an apparent contact angle. The driving force parallel to the interface of SCSA, $\tau_{SL} + \tau_{LV}\cos\theta^*_+$, increases until the maximum resistance that the SCSA can provide, defined as the $\tau_{S//,\,max}$. Afterward, the liquid corner near the three-phase contact line starts to move [bottom four panels in Fig. 4(a)]. In fact, the sole slant ratchets under vertical vibration cannot endow the substrate with a capacity for directional droplet transport [Fig. S1 and Movies S7 and S8 (supplementary material)].

From the top view, we can clearly observe an obvious change in the contact area of the droplet with the SCSA [Fig. 4(b)]. A droplet

deposited on a perfectly isotropic horizontal interface is stretched or compressed symmetrically, and the mass center would not move horizontally due to the force balance. In fact, we introduce circular arc arrays that are asymmetric thus inducing various releasing forces at liquid corners. The circular arc arrays provide continuous pinning of liquid corners along the left and right droplet edges while the actual pinning only occurs at the right edge due to the longer length of the contact line. Therefore, the droplet experiences a net forward force during vertical vibration. The overall adhesive resistance force (ΔF_r) difference of droplet transport on the SCSA along the two opposite directions can be expressed as

$$\Delta F_r = k_+\gamma\left[(l_4 - l_3) - (l_2 - l_1)\right]\cos\theta, \quad (1)$$

where k_+ is the pre-factor based on the droplet shape, γ is the SCSA-droplet interface tension, l_I (I = 1, 2, 3, and 4) is the contact line length of the droplet at the left and right edges in the stretching and compressing states, and θ is the droplet contact angle.

In contrast to vertical vibration, there is no obvious change in contact line under horizontal vibration and the overall adhesive resistance force is insufficient to overcome the pinning effect to enable directional transport [Figs. 4(e) and 4(f)]. However, the horizontal inertial driving force arising from the relative motion of droplets corresponds to the horizontally vibrated SCSA substrate. By transforming the composited movement of droplet motion and the substrate motion into the sole droplet motion corresponding to the fixed SCSA substrate, we deduce a horizontal inertial driving force (F_d), which is isotropic and periodical: $F_d = -ma = -4\pi^2 mf^2 A_0 \sin(2\pi ft + \varphi)$, where m is the mass of droplet, a is the accelerated speed of reference frame, f is the vibration frequency, A_0 is the amplitude of vibration, and φ is the initial phase of vibration. The resistance force difference ($\Delta F_{resistance}$) of droplet transport on the SCSA along the two directions could be expressed as

$$\Delta F_{resistance} = k_-\gamma R[(\cos\theta_{r1} - \cos\theta_{a1}) - (\cos\theta_{r2} - \cos\theta_{a2})]. \quad (2)$$

Here, k_- denotes the pre-factor depending on the droplet shape under horizontal vibration, R denotes the interface tension, and θ_{ri} and θ_{ai} are the receding and advancing contact angles of a droplet on the SCSA along two different directions the same as ($I = 1$) or opposed to ($I = 2$) ratchets' direction. Overall, the two distinct structures, macro millimeter-scale circular arc arrays and micro/nanometer-scale slant ratchets, play an important role in droplet motion under the vertical and horizontal vibration due to the cross-scale effect, respectively [Fig. S2 and Movies S9 and S10 (supplementary material)].

The steering transport of omni-droplets on the SCSA mediated by bi-directional vibration can be utilized for various potential applications, such as circuit on/off. In Fig. 5(a), a conductive droplet (dyed

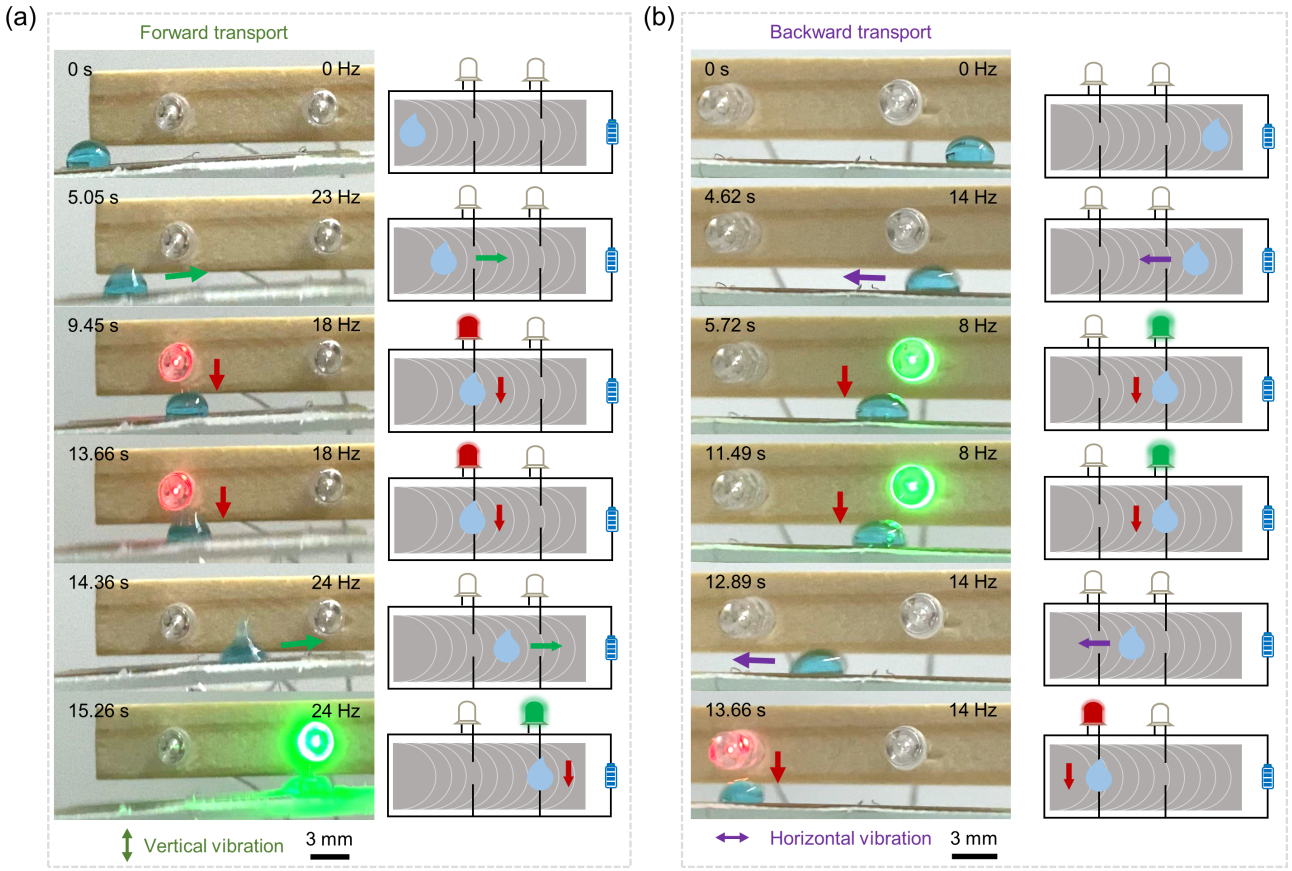

FIG. 5. (a) Under vertical vibration, a conductive droplet composed of water and NaCl with a mass fraction of 40:1 is transported along the forward direction. (b) Under horizontal vibration, the conductive droplet moves in the backward direction.

blue) is deposited on the SCSA, which is covered with a circuit consisting of two branches containing a light bulb, respectively. The conductive droplet is a liquid mixture of water and NaCl with a mass fraction of 40:1. Under vertical vibration, the droplet is driven to move in a forward transport. As the droplet goes by the first branch, the circuit is switched to be "on" state, which is characterized by the lighting red bulb. When the droplet reaches the second branch, the green bulb turns to the lighting [Movie S11 (the supplementary material)]. Similarly, under the horizontal vibration, the droplet is transported in a backward direction and the two colored bulbs are lighted up sequentially to be green and red, respectively [Fig. 5(b) and Movie S12 (the supplementary material)]. The above steering behavior of conductive droplets is of efficient potential in the reversible circuit on/off only if we utilize a composited vibrator that can acquire vertical and horizontal vibrations.

In summary, we have designed and demonstrated the steering of omni-droplets by bi-directional mechanical vibration on the slippery cross-scale arrays (SCSA). The active droplets steering by vertical or horizontal vibration have some advantages like high speed, high capacity, and programmability. The high capacity of droplet transport is achieved with this strategy, such as a high-speed velocity (>60 mm/s) and versatile manipulation range (frequency: 10–70 Hz and amplitude: 2–20 Vpp). By applying a real-time adjustable vibration frequency, multi-droplets with different volumes could be manipulated directionally in a sequential way to achieve a droplet mixing that might be used in the fields of chemical reaction and blood testing. Therefore, our work demonstrates that the SCSA under bi-directional vibration can be smartly harnessed to achieve an impressive active steering of droplets, which might open an available and complementary method for a wide range of potential applications including fluidic circuit and droplet microfluidics.

See the supplementary material for the experimental section, steering transport of water droplets on the SCSA, programmable and sequential steering manipulation of multiple droplets with different volumes, and applications, such as circuit on/off.

This work was supported by the National Natural Science Foundation of China (Grant Nos. 51875160 and 52175396), the Fundamental Research Funds for the Central Universities (Grant Nos. PA2020GDSK0077 and JZ2022HGPA0312), the National Key R&D Program of China (Grant No. JZ2022ZDYF0411), and the Opening Project of the Key Laboratory of Bionic Engineering (Ministry of Education), Jilin University. The authors would acknowledge the Experimental Center of Engineering and Material Sciences at USTC for the fabrication and measurement of samples. The financial support to L. W. from the Research Grants Council of Hong Kong (GRF 17205421, 17204420, 17210319, 17204718, and CRF C1006-20WF) is gratefully acknowledged.

AUTHOR DECLARATIONS

Conflict of Interest

The authors have no conflicts to disclose.

Author Contributions

Sizhu Wu: Conceptualization (equal); Data curation (equal); Formal analysis (equal); Funding acquisition (equal); Investigation (equal); Methodology (equal); Project administration (equal); Resources (equal); Software (equal); Supervision (equal); Validation (equal); Visualization (equal); Writing – review & editing (equal). **Yunlong Jiao:** Supervision (equal); Writing – review & editing (equal). **Chao Chen:** Data curation (equal); Writing – original draft (equal); Writing – review & editing (equal). **Zhaoxin Lao:** Supervision (equal); Writing – original draft (equal). **Liqiu Wang:** Conceptualization (equal); Investigation (equal); Supervision (equal); Writing – original draft (equal). **Le Xiang:** Conceptualization (equal); Data curation (equal); Formal analysis (equal); Investigation (equal); Methodology (equal); Writing – original draft (equal). **Yiyuan Zhang:** Conceptualization (equal); Data curation (equal); Formal analysis (equal); Methodology (equal); Supervision (equal); Validation (equal); Visualization (equal); Writing – review & editing (equal). **Shaojun Jiang:** Supervision (equal); Validation (equal); Writing – review & editing (equal). **Chuanzong Li:** Supervision (equal); Validation (equal); Writing – review & editing (equal). **Zhipeng Zhao:** Supervision (equal); Validation (equal); Writing – original draft (equal); Writing – review & editing (equal). **Yiyuan Zhang:** Writing – review & editing (equal). **Qiyu Deng:** Visualization (equal); Writing – review & editing (equal). **Shuting Xie:** Formal analysis (equal); Writing – review & editing (equal).

DATA AVAILABILITY

The data that support the findings of this study are available from the corresponding authors upon reasonable request.

REFERENCES

[1]R. Seemann, M. Brinkmann, T. Pfohl, and S. Herminghaus, "Droplet based microfluidics," Rep. Prog. Phys. **75**, 016601 (2012).
[2]K. C. Park, P. Kim, A. Grinthal, N. He, D. Fox, J. C. Weaver, and J. Aizenberg, "Condensation on slippery asymmetric bumps," Nature **531**, 78–82 (2016).
[3]Y. Zheng, H. Bai, Z. Huang, X. Tian, F. Q. Nie, Y. Zhao, J. Zhai, and L. Jiang, "Directional water collection on wetted spider silk," Nature **463**, 640–643 (2010).
[4]L. Frenz, A. E. Harrak, M. Pauly, S. Bégin-Colin, A. D. Griffiths, and J. C. Baret, "Droplet-based microreactors for the synthesis of magnetic iron oxide nanoparticles," Angew. Chem., Int. Ed. **47**, 6817–6820 (2008).
[5]W. H. Tan and S. Takeuchi, "Timing controllable electrofusion device for aqueous droplet-based microreactors," Lab Chip **6**, 757–763 (2006).
[6]Y. Zhang, J. Li, L. Xiang, J. Wang, T. Wu, Y. Jiao, S. Jiang, C. Li, S. Fan, J. Zhang, H. Wu, Y. Zhang, Y. Bian, K. Zhao, Y. Peng, W. Zhu, J. Li, Y. Hu, D. Wu, J. Chu, and Z. Wang, "A biocompatible vibration-actuated omni-droplets rectifier with large volume range fabricated by femtosecond laser," Adv. Mater. **34**, 2108567 (2022).
[7]C. J. Huang, W. F. Fang, M. S. Ke, H. Y. E. Chou, and J. T. Yang, "A biocompatible open-surface droplet manipulation platform for detection of multinucleotide polymorphism," Lab Chip **14**, 2057–2062 (2014).
[8]G. Huang, M. Li, Q. Yang, Y. Li, H. Liu, H. Yang, and F. Xu, "Magnetically actuated droplet manipulation and its potential biomedical applications," ACS Appl. Mater. Interfaces **9**, 1155–1166 (2017).
[9]S. Feng, P. Zhu, H. Zheng, H. Zhan, C. Chen, J. Li, L. Wang, X. Yao, Y. Liu, and Z. Wang, "Three-dimensional capillary ratchet-induced liquid directional steering," Science **373**, 1344–1348 (2021).
[10]H. Chen, P. Zhang, L. Zhang, H. Liu, Y. Jiang, D. Zhang, Z. Han, and L. Jiang, "Continuous directional water transport on the peristome surface of *Nepenthes alata*," Nature **532**, 85–89 (2016).
[11]Q. Wang, X. Yao, H. Liu, D. Quéré, and L. Jiang, "Self-removal of condensed water on the legs of water striders," Proc. Natl. Acad. Sci. U. S. A. **112**, 9247–9252 (2015).
[12]K. H. Chu, R. Xiao, and E. N. Wang, "Uni-directional liquid spreading on asymmetric nanostructured surfaces," Nat. Mater. **9**, 413–417 (2010).

[13]H. Chen, T. Ran, Y. Gan, J. Zhou, Y. Zhang, L. Zhang, D. Zhang, and L. Jiang, "Ultrafast water harvesting and transport in hierarchical microchannels," Nat. Mater. **17**, 935–942 (2018).
[14]M. Prakash, D. Quéré, and J. W. Bush, "Surface tension transport of prey by feeding shorebirds: The capillary ratchet," Science **320**, 931–934 (2008).
[15]M. K. Chaudhury and G. M. Whitesides, "How to make water run uphill," Science **256**, 1539–1541 (1992).
[16]J. C. Bird, S. Mandre, and H. A. Stone, "Short-time dynamics of partial wetting," Phys. Rev. Lett. **100**, 234501 (2008).
[17]Q. Sun, D. Wang, Y. Li, J. Zhang, S. Ye, J. Cui, L. Chen, Z. Wang, H. J. Butt, D. Vollmer, and X. Deng, "Surface charge printing for programmed droplet transport," Nat. Mater. **18**, 936–941 (2019).
[18]X. Li, P. Bista, A. Z. Stetten, H. Bonart, M. T. Schür, S. Hardt, F. Bodziony, H. Marschall, A. Saal, X. Deng, R. Berger, S. A. L. Weber, and H. J. Butt, "Spontaneous charging affects the motion of sliding drops," Nat. Phys. **18**, 713–720 (2022).
[19]C. Liu, C. Lu, Z. Yuan, C. Lv, and Y. Liu, "Steerable drops on heated concentric microgroove arrays," Nat. Commun. **13**, 3141 (2022).
[20]S. Daniel and M. K. Chaudhury, "Rectified motion of liquid drops on gradient surfaces induced by vibration," Langmuir **18**, 3404–3407 (2002).
[21]S. Daniel, S. Sircar, J. Gliem, and M. K. Chaudhury, "Ratcheting motion of liquid drops on gradient surfaces," Langmuir **20**, 4085–4092 (2004).
[22]S. Daniel, M. K. Chaudhury, and P. G. De Gennes, "Vibration-actuated drop motion on surfaces for batch microfluidic processes," Langmuir **21**, 4240–4248 (2005).
[23]Y. Zhang, Y. Jiao, C. Li, C. Chen, J. Li, Y. Hu, D. Wu, and J. Chu, "Bioinspired micro/nanostructured surfaces prepared by femtosecond laser direct writing for multi-functional applications," Int. J. Extreme Manuf. **2**, 032002 (2020).
[24]D. Wu, Z. Zhang, Y. Zhang, Y. Jiao, S. Jiang, H. Wu, C. Li, C. Zhang, J. Li, Y. Hu, G. Li, J. Chu, and L. Jiang, "High-performance unidirectional manipulation of microdroplets by horizontal vibration on femtosecond laser-induced slant microwall arrays," Adv. Mater. **32**, 2005039 (2020).
[25]Y. Zhang, Y. Jiao, C. Chen, S. Zhu, C. Li, J. Li, Y. Hu, D. Wu, and J. Chu, "Reversible tuning between isotropic and anisotropic sliding by one-direction mechanical stretching on microgrooved slippery surfaces," Langmuir **35**, 10625–10630 (2019).
[26]Y. Su, L. Chen, Y. Jiao, J. Zhang, C. Li, Y. Zhang, and Y. Zhang, "Hierarchical hydrophilic/hydrophobic/bumpy Janus membrane fabricated by femtosecond laser ablation for highly efficient fog harvesting," ACS Appl. Mater. Interfaces **13**, 26542–26550 (2021).
[27]T. S. Wong, S. H. Kang, S. K. Tang, E. J. Smythe, B. D. Hatton, A. Grinthal, and J. Aizenberg, "Bioinspired self-repairing slippery surfaces with pressure-stable omniphobicity," Nature **477**, 443–447 (2011).
[28]M. V. Berry, "The molecular mechanism of surface tension," Phys. Educ. **6**, 79 (1971).
[29]A. Marchand, J. H. Weijs, J. H. Snoeijer, and B. Andreotti, "Why is surface tension a force parallel to the interface?," Am. J. Phys. **79**, 999 (2011).
[30]J. Fan, J. De Coninck, H. Wu, and F. Wang, "Microscopic origin of capillary force balance at contact line," Phys. Rev. Lett. **124**, 125502 (2020).